Spin Decay, Spin-Precession Damping, and Spin-Axis Drift of the *Telstar* Satellite

By E. Y. YU

(Manuscript received March 6, 1963)

Dynamical problems of the spin-stabilized Telstar satellite, characterized by spin decay, spin-precession damping, and spin-axis drift, are analyzed in this paper. Both the eddy-current torques and the magnetic torques, which cause the above three phenomena, are evaluated. By extrapolation from the observed data, the characteristic time of the nearly exponential spin decay of the satellite is estimated to be about 330 days. A linear analysis of the precession damper is made, and the results are compared with experiments, showing that the satellite precession angle will diminish by a factor of e in a maximum time of 30 minutes. A qualitative description is given to illustrate the fundamental mechanism of spin-axis drift. Results of these analyses can be applied to any spin-stabilized satellite.

I. INTRODUCTION

For spin stabilization of a communications satellite, it is required that the satellite be statically and dynamically balanced so as to make the principal axis of maximum moment of inertia coincide with the axis of symmetry of the antenna pattern, about which the satellite is given an initial spin. This principal axis, referred to henceforth as the spin axis, is in line with the invariant angular momentum vector and is thus fixed in direction, as desired, in an inertial space, provided there are no external torques acting on the spinning satellite. However, as the satellite is spinning and traveling in the geomagnetic field, eddy-current and magnetic torques continuously act on the satellite so that the angular momentum changes its magnitude and direction, as characterized by spin decay and spin precession. As a consequence of spin decay, the satellite becomes less stable for the same external disturbing torques, and a tumbling motion may eventually result. The precession of the spin axis about the instantaneous angular momentum vector will cause wobbling of the antenna

pattern, indicating that the precession should necessarily be dissipated by means of a damping mechanism. Because of the continuous action of the torques, the angular momentum continuously changes its direction in the inertial space; meanwhile, the spin axis precesses about it and, due to the precession damping, tends to align with it. Thus, there results a gradual drift in direction of the spin axis (sometimes called long-term precession), as already observed on the Telstar satellite.

The above dynamics problems of the satellite — namely, spin decay, spin-precession damping, and spin-axis drift — are studied in this paper. In the discussion of spin decay, we will indicate the nature of the retarding torques resulting from eddy currents and magnetic hysteresis losses, analyze the observed spin decay phenomenon, and compute the $1/e$ characteristic time of the exponential decay. For the spin precession, a linear analysis of the precession damping mechanism will be given, and an experimental comparison of the damping time will be outlined. Only a short descriptive analysis is given to the problem of spin-axis drift, since an exact evaluation of the rate and pattern of drift deserves a separate computer study.

It is shown in the following that whenever a spinning rigid body undergoes energy losses (e.g., from internal friction) the axis of maximum moment of inertia or the spin axis, $\hat{z}$, and the angular velocity, $\boldsymbol{\omega}$, will tend to align with the angular momentum, $\mathbf{J} = \boldsymbol{\Phi} \cdot \boldsymbol{\omega}$, where

$$\boldsymbol{\Phi} = I_x \hat{x}\hat{x} + I_y \hat{y}\hat{y} + I_z \hat{z}\hat{z}$$

($\hat{x}$, $\hat{y}$, and $\hat{z}$ are the unit vectors along the principal axes) is the moment of inertia dyadic. If I_z of the spin axis is the minimum, the spinning motion is still stable; however, any energy dissipation will not reduce precession but make the spin axis deviate away from $\mathbf{J}$. A simple proof of the above is given in the following. The kinetic energy, E, of a spinning satellite with precession is written as

$$2E = \boldsymbol{\omega} \cdot \boldsymbol{\Phi} \cdot \boldsymbol{\omega}. \tag{1}$$

By substituting $\mathbf{J} = \boldsymbol{\Phi} \cdot \boldsymbol{\omega}$ and $\boldsymbol{\omega} = \mathbf{J} \cdot \boldsymbol{\Phi}^{-1}$ into the above, E can be expressed in terms of the angular momentum,

$$\mathbf{J} = J(\cos \xi \hat{x} + \cos \eta \hat{y} + \cos \theta \hat{z}),$$

where $\cos \xi$, $\cos \eta$, and $\cos \theta$ are the direction cosines of $\mathbf{J}$ in the body coordinates

$$2E = \mathbf{J} \cdot \boldsymbol{\Phi}^{-1} \cdot \mathbf{J} = J^2 \left(\frac{1}{I_x} \cos^2 \xi + \frac{1}{I_y} \cos^2 \eta + \frac{1}{I_z} \cos^2 \theta \right) \tag{2}$$

or, as $\cos^2 \theta = (1 - \cos^2 \xi - \cos^2 \eta)$

$$2E = J^2 \left[\frac{1}{I_z} + \left(\frac{1}{I_x} - \frac{1}{I_z} \right) \cos^2 \xi + \left(\frac{1}{I_y} - \frac{1}{I_z} \right) \cos^2 \eta \right]. \quad (3)$$

If there exists energy dissipation at a rate assumed to be so slow as to produce no torque on the satellite, the torque-free rigid body motion of the satellite will tend toward the state of minimum energy. It is observed from (2) and (3) that the minimum kinetic energy state occurs at $\theta = 0°$ (or $\xi \equiv \eta \equiv 90°$) for $I_z > I_x, I_y$, or at $\theta = 90°$ (either $\xi \equiv 0$ or $\eta \equiv 0$) for $I_z < I_x, I_y$. This proves that in order to reduce the precession angle, θ, by means of energy dissipation, I_z of the spin axis should be the maximum.

II. SPIN DECAY

Spin decay results from energy losses in the form of both eddy currents and magnetic hysteresis when the satellite is spinning in the geomagnetic field. It is shown in the following that the hysteresis losses in the magnetic materials are much smaller than the eddy-current losses in the conducting materials at high spin rates simply because the geomagnetic field in the Telstar satellite orbit is relatively weak, ranging from 0.04 to 0.4 oersted.* Magnetic materials are contained in the nickel-cadmium cells of the battery, the magnetic shielding on circuit components, etc. No measurement of the magnetic hysteresis loops has been made on the components actually used in the satellite. However, measurements on similar components contemplated for use on a proposed satellite prior to the Telstar satellite have been made, based on which it was estimated (for different orbit parameters and a different spin-axis attitude from those of the Telstar satellite) that the time-average hysteresis loss is $W = 1.6$ ergs per cycle of rotation. It is believed that the above value can be used for a conservative estimate of spin-decay rate for the Telstar satellite because it contains less magnetic materials than had been anticipated. According to this value of W, the spin decay of the satellite due to hysteresis losses alone is only about 1.5 rpm per year.

Eddy currents are generated essentially in the following parts: (a) the aluminum shell of the electronics chassis, (b) the frames of square magnesium tubing and equatorial antennas, and (c) the magnesium chassis frame assembly. An estimate of the eddy-current torque can be made if the electronics chassis is approximated as a thin spherical shell and the

* These figures are based on a spherical harmonic representation of the geomagnetic field with Hensen and Cain coefficients for the Epoch, 1960.

last two items in the above are approximated as circular loops of wire. The eddy-current torque acting on a thin spherical shell spinning at an angular velocity $\boldsymbol{\omega}$ can be shown to be

$$\mathbf{T}_1 = p_1\mathbf{B} \times (\mathbf{B} \times \boldsymbol{\omega}) \tag{4}$$

where $\mathbf{B}$ is the geomagnetic induction and $p_1 = (2\pi/3)a^4\sigma\, d$, with a = radius, d = thickness, and σ = volume conductivity. The above expression is correct only when the square of the nondimensional quantity, $\frac{1}{3}\mu a\sigma\omega d$ (μ = free-space permeability), is negligibly small compared to unity, which is found to be true in the present case. The above torque can be resolved into two components, i.e., the component parallel to $\boldsymbol{\omega}$

$$T_{\parallel} = -p_1 B_{\perp}^{\,2}\omega \tag{5}*$$

which tends to retard ω($B_{\perp}$ = component of $\mathbf{B}$ normal to $\boldsymbol{\omega}$) and the component normal to $\boldsymbol{\omega}$

$$T_{\perp} = p_1 B_{\parallel} B_{\perp}\omega \tag{6}$$

which contributes to the precession of the satellite ($B_{\parallel}$ = component of $\mathbf{B}$ parallel to $\boldsymbol{\omega}$). In the case of a circular loop, it can be easily shown that the time-average eddy-current torque, acting on a circular loop spinning about a diameter, tends only to retard $\boldsymbol{\omega}$; i.e.

$$\mathbf{T}_2 = -p_2 B_{\perp}^{\,2}\boldsymbol{\omega} \tag{7}$$

where $p_2 = A^2/2R'$ (A = loop area, $R' = l'/\sigma A_w$ = total resistance of the loop of wire, A_w = cross-sectional area of the wire, l' = length of the loop). The above expression is correct only when the square of the nondimensional quantity, $\omega L'/R'$ (L' = inductance), is negligibly small compared to unity, which is found to be the case here. The other component normal to $\boldsymbol{\omega}$ has a zero time-average value.

In general, the eddy-current retarding torque acting on a conducting body spinning in a magnetic field is proportional to $B_{\perp}^{\,2}$ and ω, or can be written approximately as

$$\mathbf{T}_r = -pB_{\perp}^{\,2}\boldsymbol{\omega} \tag{8}$$

where p is a constant and is determined by the conducting material and its geometry. Thus, for the Telstar satellite, if the electronics chassis is approximated as a thin spherical shell (of 9.5-inch radius and 0.1-inch thickness) and the frames are approximated as circular loops of wire, then the retarding torque, T_r, acting on the satellite is the sum of $T_{\parallel}$ in

* This expression is the same as that given in Ref. 1, p. 417, problem 12, after the square of the nondimensional quantity, $\frac{1}{3}\mu a\sigma\omega d$, is neglected.

(5) and T_2 in (7) or $p = p_1 + p_2$. It is calculated that $p_1 = 684$, $p_2 = 256$, or $p = 940$ meter^4/ohm in mks units. This value of p is of course too low, because many small conducting parts have not been considered in the calculation. From the expressions of p_1 and p_2, one notices that p_1 is proportional to the fourth power of the radius of a spherical shell and p_2 to the square of the loop area. For this reason, the Telstar satellite was insulated at the equatorial antennas in such a way that the outer shell does not constitute a large continuous surface and that the frames do not form large continuous loops.

The magnitude of p in (8) for the Telstar satellite can be measured by rotating a magnetic field normal to the spin axis while the angular deflection of a torsion wire, which suspends the satellite along the spin axis, is recorded to determine the drag torque. Such an experiment has been devised by M. S. Glass and D. P. Brady. Measurements made on the prototype give $p = 1355$ meter^4/ohm $\pm$ 15 per cent. This measured value is believed to be somewhat high, because the magnetic field applied in the measurements was as high as 25 to 100 oersteds (at 23.4 rpm) in order to give significant angular deflection readings of the suspension wire; thus, the measured drag torque unavoidably includes losses due to full hysteresis loops described in the magnetic materials. In the actual case, the magnetic field along the orbit is only 0.04–0.4 oersted, and the losses due to minor hysteresis loops are much smaller. Besides, since the electromagnetic characteristics of the satellite may be different from one model to another, the value of p measured on the prototype may not be applied to the Telstar satellite with good accuracy. Nevertheless, it is believed that the value of p in meter^4/ohm is bounded below by 940 and above by 1560. A later calculation by extrapolation from the observed data on the satellite showed that p is approximately equal to 1110. A further refinement of the evaluation of p might have been obtained from the instantaneous spin-decay rate which can be determined from the telemetry solar aspect data. However, as the obtained instantaneous spin-decay rate was too low to give any significant reading, such an attempt failed to yield any results.

Because of proper functioning of the precession damper, the Telstar satellite is now spinning nearly about its principal z-axis of maximum moment of inertia. In this case, $B_\perp$ in (8) can be approximated as the component of B normal to the z-axis. Obviously, $B_\perp$ is a function of time due to (a) the rotation of the slightly inclined geomagnetic field about the earth's spin axis, (b) the anomalies of the geomagnetic field, (c) the gradual drift in direction of the satellite spin axis, and (d) the variation of orbital parameters due to the oblateness of the earth, notably the apsidal advance and the nodal regression (see Fig. 1). For the same rea-

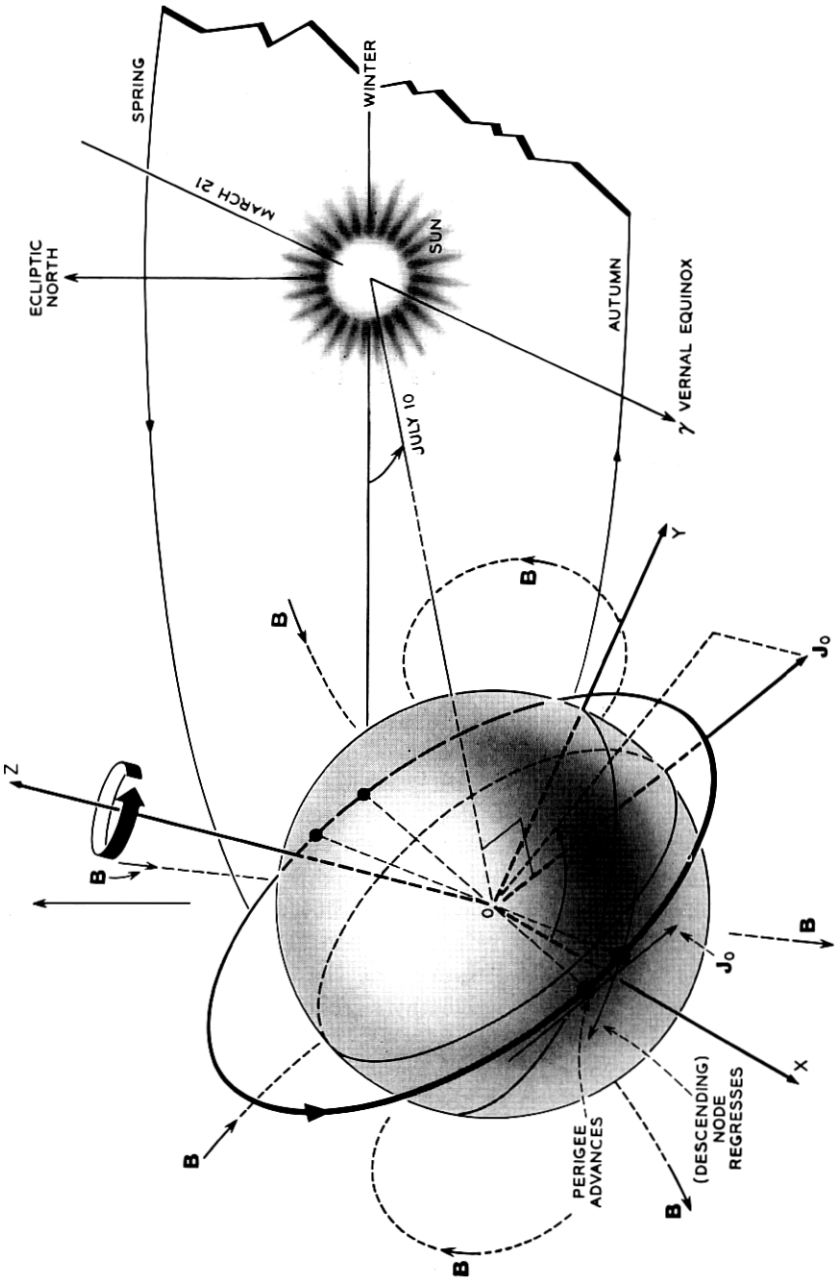

Fig. 1 — Initial Telstar satellite orbit in nonrotating coordinates, O-XYZ.

sons, the magnetic hysteresis loss per cycle of rotation, W, is also a function of time. The decay of spin rate due to both eddy-current and hysteresis losses can be determined from the following equation

$$I_z\dot{\omega} = -pB_\perp^2(t)\omega - \frac{1}{2\pi}W(t) \tag{9}$$

or, upon integration,

$$\omega = \exp\left(-\int_0^t (p/I_z)B_\perp^2(t)\,dt\right) \cdot\left[\omega_0 - \int_0^t \frac{W(t)}{2\pi I_z}\exp\left(\int_0^t (p/I_z)B_\perp^2(t)\,dt\right)dt\right] \tag{10}$$

where $\omega_0 = \omega(t = 0)$. Let us now define day-average values $\overline{B_\perp^2}$ and $\overline{W}$ as

$$\overline{B_\perp^2} = \frac{1}{t}\int_0^t B_\perp^2(t)\,dt \tag{11}$$

and

$$\overline{W} = \frac{\int_0^t W(t)\exp\left(\int_0^t (p/I_z)B_\perp^2(t)\,dt\right)dt}{\int_0^t \exp\left(\int_0^t (p/I_z)B_\perp^2(t)\,dt\right)dt}. \tag{12}$$

Then (10) can be written as

$$\omega = \left[\omega_0 + \frac{1}{2\pi}\frac{\overline{W}(t)}{p\overline{B_\perp^2}(t)}\right]e^{-t/\tau} - \frac{1}{2\pi}\frac{\overline{W}(t)}{p\overline{B_\perp^2}(t)} \tag{13}$$

where

$$\tau = I_z/p\overline{B_\perp^2}(t). \tag{14}$$

The time t in (13) is in units of days, and $\overline{B_\perp^2}(t)$ and $\overline{W}(t)$ are functions of t. Note that if the term $\overline{W}/2\pi p\overline{B_\perp^2}$, which is much smaller than ω_0 in the case of the Telstar satellite, is neglected in (13), the spin decay is exponential with time with, however, a time-dependent τ.

A plot of $\overline{B_\perp^2}(t)$ is given in Fig. 2 from the day of launch (July 10, 1962) up to December 31, 1962. The day-average $\overline{B_\perp^2}(t)$ is obtained by taking the arithmetic mean of the time-average values of $B_\perp^2$ per pass for approximately nine passes a day. The latter values are computed*

* Computations were provided by J. D. Gabbe.

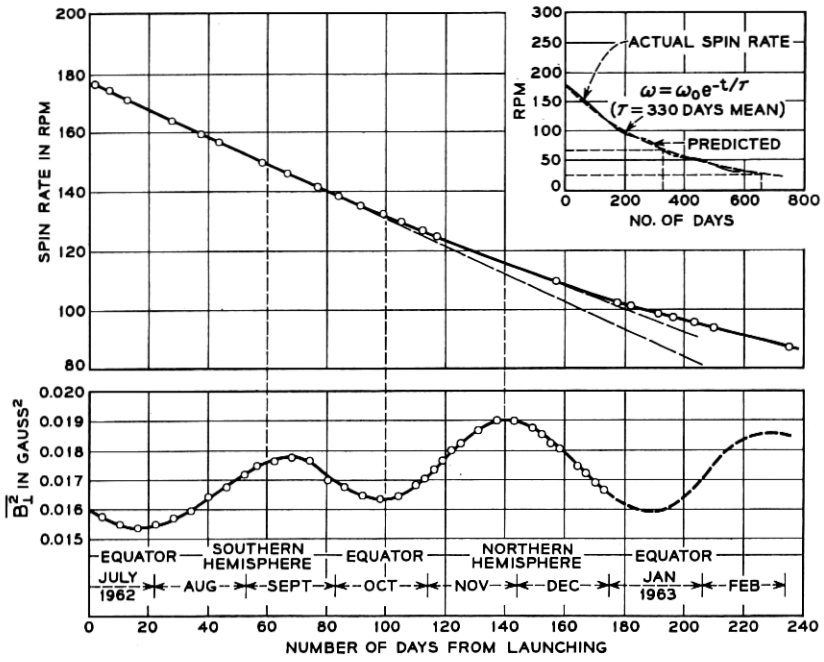

Fig. 2 — Spin rate and $\overline{B_\perp^2}$ vs time.

from a spherical harmonic representation of the geomagnetic field, taking into account the continuous variations of the spin-axis direction and of the orbital parameters. Because of these combined effects, the variation of $\overline{B_\perp^2}$ is sinusoidal with time with, however, variable amplitude and period. The major contribution to this variation is believed to be due to the apsidal advance in the orbital plane. In order to see this, let us plot in Fig. 3 the time-average values of $B_\perp^2$ per pass versus the geographical longitude of the perigee in the beginning of the pass on the days of July 15, 18 and 21, 1962. The latitudes of the perigee on those three days were $\pm 5°$ within the geographical equator. It is shown on these curves that $B_\perp^2$ is relatively low when the perigee falls in the region over South America where the geomagnetic field strength is depressed. The center of this region falls at approximately 25°S latitude and 45°W longitude. (See Ref. 2 for details.) Fig. 3 is a typical example, which shows how the magnitude of $B_\perp^2$ depends critically on the position of perigee, although the variation of $B_\perp^2$, which also depends on other factors as previously stated, does not necessarily follow the same pattern as in Fig. 3 when the perigee is in other positions. At any rate,

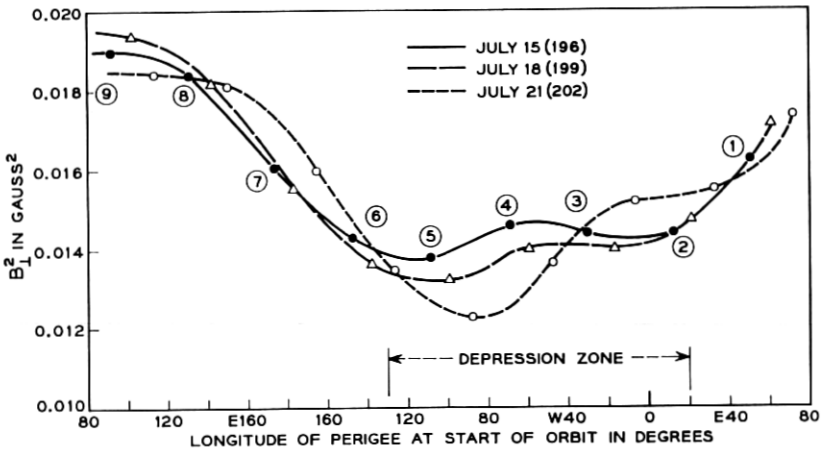

Fig. 3 — $B_\perp^2$ vs longitude of perigee at start of orbit.

the change of position of the perigee is a determining factor for the variation of the day-average $\overline{B_\perp^2}$ and of the observed* spin-rate curve, as plotted in Fig. 2. The initial perigee of the Telstar satellite orbit (593 miles in altitude) was north of the geomagnetic equator on the day of launch, as indicated in Fig. 1. The perigee advances in the direction of the orbital motion at a rate of approximately 2° per day. When the perigee was crossing the geomagnetic equator southward in the orbital plane, $\overline{B_\perp^2}$ first decreased and then increased, as indicated in the initial part of the $\overline{B_\perp^2}$ curve in Fig. 2. In the ascending part of the curve up to September 7, 1962, $t = 60$ days, more spin decay occurred than would result from an exponential decay produced by a constant $\overline{B_\perp^2}$ when the perigee was over the equator. This is why the corresponding part of the spin-rate plot is nearly a straight line instead of an exponential decay curve. From $t = 60$ days to $t = 100$ days, while the perigee was advancing northward toward the geomagnetic equator, $\overline{B_\perp^2}$ was leveling off and then declining, resulting in an exponential decay as shown in the part of the spin-rate plot deviating from the extension of the straight line. From $t = 100$ days to $t = 140$ days, the perigee was entering the northern hemisphere, again getting into a stronger geomagnetic field indicated by the increasing $\overline{B_\perp^2}$. As a result, this part of the spin-rate curve becomes nearly a straight line again, though of a dif-

* The spin rate of the Telstar satellite was measured by J. S. Courtney-Pratt and his coworkers by means of the glint method (see Ref. 3 for details). It was also determined by C. C. Cutler and W. C. Jakes by way of measuring the frequency of the ripple in the amplitude of the radio signal received from the satellite.

ferent slope than the first one. Then the spin decay became exponential again when the perigee was moving southward toward the equator from $t = 140$ to $t = 190$ days. All these indicate that the actual spin-rate curve would wiggle about a mean exponential curve as shown in Fig. 2. Note from Fig. 2 that $\overline{B_\perp{}^2}$ is lower when the perigee is in the southern hemisphere. This is due to the zone of depressed geomagnetic field strength previously mentioned. It is believed that, as the perigee keeps advancing in the orbital direction, $\overline{B_\perp{}^2}(t)$ will continue to vary sinusoidally with time. Nevertheless, complete values of $\overline{B_\perp{}^2}$ cannot be predicted for the entire useful life of the satellite because the spin axis changes its direction continuously because of perturbation of the electromagnetic torques as well as occasional operation of the torque coil,* and because variation of the orbital parameters cannot be predicted accurately. Therefore, exact evaluation of the $1/e$ characteristic time of the nearly exponential spin decay cannot be obtained. Nevertheless, it may be approximately evaluated as follows.

First, let us determine the value of p of the Telstar satellite from the observed spin-decay rate in the first 35 days, which is practically linear with time, with $\omega_0 = 18.67$ rad/sec (178.33 rpm) at $t = 0$ and $\omega = 16.9$ rad/sec (161.2 rpm) at $t = 35$ days. Let us take $\overline{B_\perp{}^2}$ and $\overline{W}$ as constants in (13) and, as t/τ is small, we may expand $\exp(-t/\tau)$ up to the first-order term in t/τ

$$\omega \approx \omega_0 \left(1 - \frac{p\overline{B_\perp{}^2}}{I_z} t\right) - \frac{1}{2\pi} \frac{\overline{W}}{I_z} t.$$

Substituting into the above with $\omega = 16.9$, $\omega_0 = 18.67$ rad/sec, $I_z = 5.61$ kg-m^2, $\overline{W} = 1.6 \times 10^{-7}$ joules, and $t = 35$ days $= 3.024 \times 10^6$ sec, we find that

$$p\overline{B_\perp{}^2} = 1.748 \times 10^{-7} \text{ weber}^2/\text{ohm}.$$

If we take $\overline{B_\perp{}^2}$ to be 1.572×10^{-10} weber^2/meter^4, then $p = 1110$ meter^4/ohm. Now, we note from Fig. 2 that $\overline{B_\perp{}^2}$ varies between 0.0154 and 0.0190 gauss^2. If we take the average value of $\overline{B_\perp{}^2}$ for the entire useful life of the Telstar satellite, denoted as $\overline{\overline{B_\perp{}^2}}$, to be 0.0177 gauss^2 $\pm$ 2 per cent, then the average $1/e$ characteristic time of the exponential spin decay without considering hysteresis losses is found to be

$$\tau = \frac{I_z}{p\overline{\overline{B_\perp{}^2}}} = 330 \text{ days} \pm 2 \text{ per cent} \qquad (15)$$

* The torque coil consists of 200 turns of 32-gauge copper wire wound around the equator of the satellite. When current is turned on at a desired time, the magnetic moment of the coil will interact with the geomagnetic induction to produce torque for correction of the spin-axis direction.

for $p = 1110$ meter^4/ohm. An exponential curve based on this mean $1/e$ time is plotted in Fig. 2; in addition, the actual spin-rate curve is also drawn (not to scale) in order to show that the latter curve is fluctuating about the mean exponential curve at a period of about 180 days. If the hysteresis losses are taken into account, the $1/e$ characteristic time is expressed as

$$\tau_h = \tau \ln [(\omega_0 + \overline{\overline{W}}/2\pi p\overline{\overline{B_\perp{}^2}})/(\omega_0/e + \overline{\overline{W}}/2\pi p\overline{\overline{B_\perp{}^2}})] \qquad (16)$$

where $\overline{\overline{W}}$ is the average value of $\overline{W}(t)$ for the entire useful life of the satellite. Let $\overline{\overline{W}}$ be 1.6 ergs per cycle of rotation for a conservative estimate, then $\tau_h = 327$ days $\pm$ 2 per cent.

Based on the above range of the exponential decay rate, the satellite will spin at about 20 rpm at the end of two years from the day of launch. If the equatorial antennas had not been insulated, a separate calculation indicates that the spin rate after two years would be only about 3 rpm, which seems too low to insure attitude stabilization.

III. SPIN PRECESSION AND PRECESSION DAMPING

Before analyzing precession damping, let us first consider precessional motion of a spinning satellite produced by torques acting transversely to the spin axis. Suppose that the satellite, assumed here to be a rigid body, is initially spinning about its z-axis so that its initial angular momentum is $\mathbf{J}_0 = I_z\boldsymbol{\omega} = I_z\omega\hat{z}$. When a transverse torque $\mathbf{T}$ is acting on the satellite for a time interval Δt, $\mathbf{J}_0$ changes to $\mathbf{J}$ by an amount $\Delta\mathbf{J}$, which is equal to the impulse $\mathbf{T}\Delta t$, as shown in Fig. 4(a). The satellite will then perform precession with the spin axis, $\hat{z}$, and the angular velocity, $\boldsymbol{\omega}$, no longer aligned with $\mathbf{J}$.

The torques causing precession consist of (a) gravitational torque, (b) eddy-current torque, and (c) torque of interaction between the residual magnetic dipole moment, $\mathbf{M}$, and the geomagnetic field, $\mathbf{H}$. The components of the gravitational torque, $3(gR_0{}^2/\rho^3)\hat{\rho} \times \boldsymbol{\Phi}\cdot\hat{\rho}$ (ρ = geocentric distance, g = gravitational acceleration at earth's surface, and R_0 = earth's radius) normal to the spin axis are proportional to $(I_z - I_x)$ or $(I_z - I_y)$ and are found to have a maximum value of 0.65×10^{-6} ft-lb at perigee of the Telstar satellite orbit (based on the measured values of $I_x = 3.7140$, $I_y = 3.8252$, and $I_z = 4.1412$ slug-ft^2). The eddy-current torque given in (6) can reach a maximum value of 0.56×10^{-6} ft-lb (for $p_1 = 684$ meter^4/ohm and $|B_\parallel B_\perp| = 0.6 \times 10^{-10}$ weber^2/meter^4). The maximum magnitude of the magnetic torque, $\mathbf{M} \times \mathbf{H}$, is as high as 13.2×10^{-6} ft-lb (for $H = 31.84$ amp-turns/m or

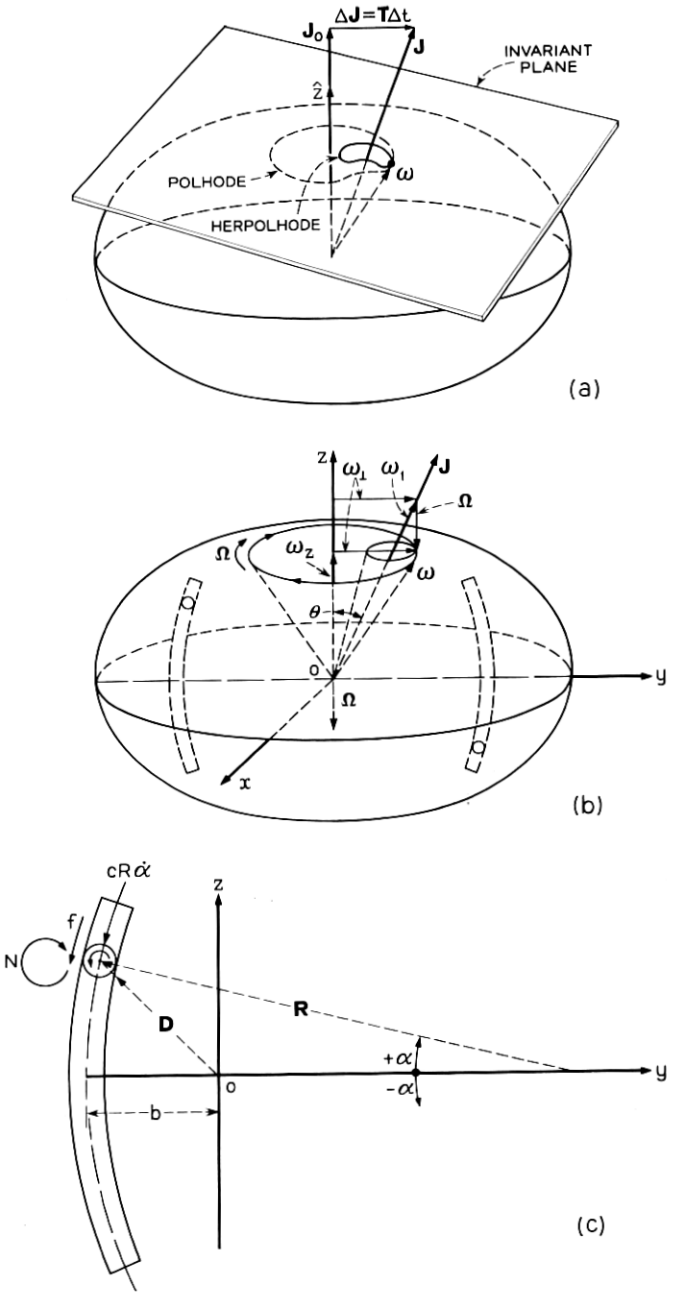

Fig. 4 — (a) Motion of Poinsot's inertia ellipsoid; (b) motion of oblate spheroidal rigid body; and (c) motion of ball in the precession damper.

0.4 oersted and $M = 0.562 \times 10^{-6}$ weber-meter*). Thus, both the gravitational and eddy-current torques are at least one order of magnitude smaller than the magnetic dipole moment torque.

For the analysis of precession damping, let us assume that **J** is temporarily an invariant, since **T** is so small (about 10^{-5} ft-lb maximum, as given above) that it takes a minimum time of about 1.5 days for **J** to change its direction by one degree, whereas the $1/e$ characteristic precession damping time, τ_p, is only of the order of 30 minutes, as will be shown later. Thus, within the time interval comparable to τ_p the precessional motion can be treated as torque-free. Such a motion can be pictured by Poinsot's geometrical construction (see Ref. 4, p. 161) in which the satellite's inertia ellipsoid rolls without slipping on the invariant plane, which is a plane normal to **J** and tangent to the ellipsoid at a fixed distance from the origin of the ellipsoid [see Fig. 4(a)]. The curve traced out by the point of contact on the ellipsoid, known as the polhode, is the locus of the tip of $\boldsymbol{\omega}$ in the body, while the curve on the invariant plane, known as the herpolhode, is the locus of the tip of $\boldsymbol{\omega}$ in the inertial space. To simplify the analysis of the precession damping, we further assume that the satellite is symmetric about its spin axis, or the inertia ellipsoid is an oblate spheroid with a transverse moment of inertia $I(=I_x = I_y) < I_z$. In this case, the precession motion can be visualized, as shown in Fig. 4(b), as a body cone, $zO\omega$, rotating at an angular velocity, $\boldsymbol{\Omega}$, on an immovable space cone, $JO\omega$, which is rotating at an angular velocity, $\boldsymbol{\omega}_1$, along the fixed direction of **J**. The line of tangency between these two cones is the instantaneous axis of rotation of the body or the angular velocity, $\boldsymbol{\omega}$, which is the sum of $\boldsymbol{\Omega}$ and $\boldsymbol{\omega}_1$. The analytic solution of such a torque-free precession motion of an oblate spheroidal body is obtained (see Ref. 4, p. 162) for the angular velocity $\boldsymbol{\omega} = \omega_x\hat{x} + \omega_y\hat{y} + \omega_z\hat{z}$ expressed in the body coordinates with components

$$\begin{aligned} \omega_x &= \omega_\perp \sin \Omega t \\ \omega_y &= \omega_\perp \cos \Omega t \\ \omega_z &= \tilde{\omega}_z (= \text{constant}) \end{aligned} \tag{17}$$

where

$$\Omega = \left(\frac{I - I_z}{I}\right) \omega_z \tag{18}$$

* Measured by M. S. Glass and D. P. Brady.

and, as is apparent from Fig. 4(b)

$$\omega_\perp = (\omega_z - \Omega) \tan \theta = \frac{I_z}{I} \omega_z \tan \theta = \text{constant.} \tag{19}$$

Here, it is obvious that the precession angle, θ, between the spin axis, $\hat{z}$, and J is a constant, providing there exists no precession energy dissipation.

The precession energy is the difference between two energy states with and without precession. We use the same assumption as in Section I: that the precession energy dissipation produces negligibly small torque to the rigid body motion. Thus, during the time interval when the precession is substantially damped out, the angular momentum can be treated as an invariant. The kinetic energy in the presence of precession is

$$E = \tfrac{1}{2} I \omega_\perp^2 + \tfrac{1}{2} I_z \omega_z^2$$

where $\omega_\perp^2 = \omega_x^2 + \omega_y^2$, and as shown in Section I the minimum energy state occurs when the precession is completely damped out, i.e.

$$E_{\min} = \tfrac{1}{2} I_z \omega_z'^2$$

where ω_z' can be found from the invariant angular momentum

$$J^2 = I^2 \omega_\perp^2 + I_z^2 \omega_z^2 = I_z^2 \omega_z'^2$$

or

$$\omega_z'^2 = \left(\frac{I}{I_z}\right)^2 \omega_\perp^2 + \omega_z^2 .$$

Therefore, the precession energy is

$$E_p = E - E_{\min} = \frac{1}{2} \left(1 - \frac{I}{I_z}\right) I \omega_\perp^2$$

or, by virtue of (19)

$$E_p = \frac{1}{2} \left(\frac{I_z}{I} - 1\right) I_z \omega_z^2 \tan^2 \theta. \tag{20}$$

Note that when $I = I_z$ for a spherical satellite there is no precession energy.

To dissipate the precession energy, the satellite is equipped with a pair of curved aluminum tubes filled with neon gas at one atmosphere,

each containing a tungsten ball of radius r and mass m [see Fig. 4(c)]. The ball is slightly smaller than the inside diameter of the tube, and the curved tubes are installed concavely towards the spin axis with their bisecting radii of curvature, R, perpendicular to the spin axis at the center of mass of the satellite. When the satellite is rotating precisely about its spin axis, the balls are stationary at the middle of the tubes. However, when precession occurs — i.e., when $\boldsymbol{\omega}$ is precessing along the body cone or following the polhode in the inertia ellipsoid — the balls are forced to move back and forth against the viscous friction of the gas as well as the inviscid friction between the balls and the tubes. Hence, the precession energy is dissipated into heat through the resistances to the motion of the balls, resulting in the attenuation of the precession angle, θ, or in the realignment of the spin axis, $\hat{z}$, and $\boldsymbol{\omega}$ with $\mathbf{J}$.

To derive the equations of motion of the ball, we assume that the ball rolls on the tube without sliding. The equation of the ball's rotational motion about its center of mass can be immediately written in terms of the angle, α, from the y-axis (the tubes are assumed to lie in the yz-plane)

$$\frac{2}{5} mr^2 \left(\frac{R}{r} \ddot{\alpha}\right) = fr - N \tag{21}$$

where f is the force acting at the point of contact, and N the resistance moment due to rolling friction. The position vector of the center of mass of the ball, as shown in Fig. 4(c), is given in the body coordinates as

$$\mathbf{D} = [R(1 - \cos \alpha) - b]\hat{y} + R \sin \alpha \hat{z}. \tag{22}$$

The equation of the translational motion of the ball is then

$$m \frac{d^2\mathbf{D}}{dt^2} \cdot \hat{q} = -f - cR\dot{\alpha} \tag{23}$$

where $\hat{q} = \sin \alpha \hat{y} + \cos \alpha \hat{z}$ is the tangential unit vector in the direction of $\dot{\alpha}$ and c the coefficient of viscous friction. In performing the differentiation of $\mathbf{D}$ with respect to time, one should be aware of the fact that the angular velocity, $\boldsymbol{\omega}$, as given in (17) in the body coordinates of a precessing body, is changing in direction in an inertial space and its time derivative is $\dot{\boldsymbol{\omega}} = \boldsymbol{\omega} \times \boldsymbol{\Omega}$, where $\boldsymbol{\Omega} = \Omega \hat{z}$. Therefore, it should be noted, for example, that $(d/dt)\hat{y} = \boldsymbol{\omega} \times \hat{y}$ and $(d^2/dt^2)\hat{y} = (\boldsymbol{\omega} \times \boldsymbol{\Omega}) \times \hat{y} + \boldsymbol{\omega} \times (\boldsymbol{\omega} \times \hat{y})$. Upon differentiating $\mathbf{D}$ in (22) twice with respect to time, substituting into (23), and using (21) to eliminate f, we obtain a nonlinear second-order equation for α

$$\ddot{\alpha} - \frac{5}{7R}\omega_z^2[R(1 - \cos\alpha) - b]\sin\alpha + \frac{5}{7}\omega_y(\omega_z - \Omega)\sin^2\alpha$$

$$- \frac{5}{7}\omega_\perp^2 \sin\alpha\cos\alpha + \frac{5}{7R}\omega_y(\omega_z + \Omega)[R(1 - \cos\alpha) - b]\cos\alpha \quad (24)$$

$$= -\frac{5c}{7m}\dot{\alpha} - \frac{\dot{\alpha}}{|\dot{\alpha}|}\frac{5N}{7mrR}$$

where the sign of N has been chosen in such a way as to make the resistance moment always oppose the rotational motion of the ball, and $\omega_y = \omega_\perp \cos\Omega t = (\omega_z - \Omega)\tan\theta\cos\Omega t$. As the radius of curvature, $R(\ = 15$ ft), of the tube used on the Telstar satellite is much larger than its length, $L(\approx 1.4$ ft), the maximum angle of α is very small, viz., $\alpha_m = L/2R = 0.0465$ radian $\ll 1$, where α_m is the subtended half angle of the curved tube. In order for the balls to move back and forth without bottoming with the ends of the tubes, the precession angle, θ, should be of the same order as α. Thus, for small α and θ, (24) can be linearized to the following

$$\ddot{\alpha} + 2n\dot{\alpha} + P^2\alpha + \frac{\dot{\alpha}}{|\dot{\alpha}|}K = q\cos\Omega t \quad (25)$$

where $2n = 5c/7m$, $P^2 = 5b\omega_z^2/7R$, $K = 5N/7mrR$, and $q = (5b/7R)\cdot\theta(\omega_z^2 - \Omega^2)$. Because of the presence of the rolling friction term, the above equation can be solved only for each half cycle.

An experiment has been conducted by the author to determine the resistance moment, N, that the tungsten ball encounters when rolling on the aluminum tube. For convenience, N is expressed in terms of a resistance force, F, acting at the center of the ball: i.e., $N = Fr$, and F is determined experimentally to be $F = 0.0002$ lb. In another experiment devised to measure the coefficient of viscous friction, c, for the 0.484-inch ball moving in the tube (nominal inside diameter $= 0.495$ in.) filled with neon gas at one atmosphere, it is found that $c = 0.00193$ lb-sec/ft. The ratio of the energy dissipation per cycle due to the viscous friction (in the steady-state forced oscillation case) and that due to the rolling friction can be shown to be $E_v/E_r = |\pi cR\Omega\alpha_m/4F|$. With $\alpha_m = 0.0465$ radian, $R = 15$ ft, $|\Omega| = 1.50$ rad/sec, corresponding to the case of the Telstar satellite at 178.33 rpm, the above ratio is about 8. This indicates that energy dissipation per cycle due to rolling friction is approximately one order of magnitude smaller than that due to viscous friction at the indicated spin rate. If the rolling friction term is neglected, (25) becomes

$$\ddot{\alpha} + 2n\dot{\alpha} + P^2\alpha = q\cos\Omega t \quad (26)$$

for which the steady-state forced oscillation solution is

$$\alpha = \alpha_0 \cos(\Omega t - \beta) \tag{27}$$

where

$$\begin{aligned} \alpha_0 &= \theta\left(1 - \frac{\Omega^2}{\omega_z^2}\right)\left[\left(1 - \frac{\Omega^2}{P^2}\right)^2 + \frac{4n^2\Omega^2}{P^4}\right]^{-\frac{1}{2}} \\ \cos\beta &= (P^2 - \Omega^2)[(P^2 - \Omega^2)^2 + 4n^2\Omega^2]^{-\frac{1}{2}} \\ \sin\beta &= 2\Omega n[(P^2 - \Omega^2)^2 + 4n^2\Omega^2]^{-\frac{1}{2}}. \end{aligned} \tag{28}$$

The energy dissipation due to viscous friction per period of oscillation of the ball (or per period of precession) is

$$E_v = \int_0^T cR^2\dot{\alpha}^2\, dt = cR^2\alpha_0^2\Omega \int_0^{2\pi} \sin^2(\Omega t - \beta)\, d(\Omega t) = \pi cR^2\alpha_0^2\Omega. \tag{29}$$

The time-average rate of energy dissipation per period of precession appears to be

$$\frac{\overline{dE_v}}{dt} = \frac{E_v}{\left(\frac{2\pi}{\Omega}\right)} = \frac{1}{2} cR^2\Omega^2\alpha_0^2. \tag{30}$$

Equating the negative of the above to the rate of change of the precessional energy, E_p, in (20) for the case of a small angle, $\tan\theta \approx \theta$, an equation for the change of the precession angle θ is obtained

$$\left(\frac{I_z}{I} - 1\right) I_z\omega_z^2\theta\dot{\theta} = -\frac{1}{2} cR^2\Omega^2\alpha_0^2. \tag{31}$$

Substituting into the above with α_0 given by (28) and integrating, we obtain an exponential decay of θ with time

$$\theta = \theta_0 e^{-t/\tau_p} \tag{32}$$

where $\theta_0 = \theta(t = 0)$ and τ_p is the characteristic time given as

$$\tau_p = \frac{5I_z}{7nmR^2(\lambda - 1)\lambda^2(2 - \lambda)^2}\left[\left(1 - \frac{\Omega^2}{P^2}\right)^2 + \frac{4n^2\Omega^2}{P^4}\right] \tag{33}$$

with $\lambda = I_z/I\,(>1)$. If the time-average rate of energy dissipation per cycle due to rolling friction, $4FR\alpha_0\,|\,\Omega\,|/2\pi$, is included in (31), the solution for θ becomes

$$\theta = (\theta_0 + h)e^{-t/\tau_p} - h \tag{34}$$

where

$$h = \frac{10F}{7\pi mnR\omega_z(\lambda - 1)\lambda(2 - \lambda)}\left[\left(1 - \frac{\Omega^2}{P^2}\right)^2 + \frac{4n^2\Omega^2}{P^4}\right]^{\frac{1}{2}}. \quad (35)$$

The $1/e$ characteristic time in this case is

$$\tau_p' = \tau_p \ln\left(\frac{1 + \frac{\theta_0}{h}}{1 + \frac{\theta_0}{he}}\right) \quad (36)$$

which involves the initial angle, θ_0. Because of the rolling friction, the precession will be damped out within a finite time, i.e., $\theta = 0$ at $t = \tau_p \ln (1 + \theta_0/h)$. A numerical computation, corresponding to the Telstar satellite physical constants, shows that h is considerably smaller than one degree. This indicates that if the precession angle, θ, is substantially greater than one degree, the $1/e$ characteristic time given in (33) for viscous friction alone should be used for convenience, since it is independent of the initial condition.

From (26) it is seen that if the natural frequency, P, is made equal to the frequency of the forcing term, Ω, i.e., if

$$R = \frac{5}{7(\lambda - 1)^2} b \quad (37)$$

then the oscillating motion of the ball is in resonance with the precession motion of the satellite. As a consequence, the $1/e$ characteristic time becomes much shorter

$$\tau_{pr} = \frac{28nI_z(\lambda - 1)}{5mb^2\lambda^2\omega_z^2(2 - \lambda)^2}. \quad (38)$$

Unfortunately, such a tuned damper cannot be obtained for the Telstar satellite, since the ratio of moments of inertia ($I/I_z = 0.897$, 0.925 or $\lambda = 1.114$, 1.08) is close to unity, and as the tubes are placed outside of the electronics package, b cannot be made too small. Therefore, in view of (37), a tuned damper for the Telstar satellite would have to be of an exceedingly large radius of curvature (R = 57–117 ft for b = 1.046 ft). In this case, the tubes become practically straight, and the motion of the balls may not necessarily be at resonance with the precession of the satellite. The equation of motion of a ball in a straight tube can be easily obtained by multiplying (26) through with R and then letting $R \to \infty$ or $P \to 0$; in a similar way, the $1/e$ characteristic time can be obtained. Nevertheless, such a straight or nearly straight tube

damper will not be used for the essential reason that, in case of its misalignment with the spin axis, no damping whatsoever will be obtained when the precession angle is smaller than the misalignment angle. Another type of damper can be obtained if the curved tube is placed concavely away from the spin axis. The equation of motion of the ball in such a tube can be easily shown to be the same as (26) except that the sign of the α term is negative, hence forming an unstable system. The ball, which rests at one end of the tube, will move toward the other end at a high speed when a component of ω is tangent to the former end of the tube and is large enough to make the centrifugal force overcome the static friction. The ball will move back and forth twice in each period of precession. Let the kinetic energy of the ball when it reaches the other end of the tube equal the centrifugal force times the distance traveled by the ball perpendicular to ω. If we assume that the kinetic energy of the ball is completely absorbed by bottoming at each end of the tube, it can be shown that the decay of the precession angle is parabolic with time. Such a damper can effectively reduce the precession even when the ratio I/I_z is close to unity, but it will not damp out a precession angle less than about three degrees; thus, it was not adopted for use with the Telstar satellite.

After comparing the advantages and disadvantages of the several dampers discussed, the untuned concave damper shown in Figs. 4(b) and (c) was finally chosen for the Telstar satellite, although its damping time is somewhat larger than that of the others. This choice was made because the theoretical $1/e$ characteristic damping time, given in (33), is calculated to be a maximum of about three minutes for a ratio of I/I_z up to 0.95, a spin-rate range of 20–180 rpm, and for the parameters given below. Such a damping time is acceptable even if it is one order of magnitude larger, in view of the slow rate of change of the angular momentum due to the small transverse torques previously calculated. The chosen parameters are: $R = 15$ ft (a large value, although the tube still has noticeable curvature), $m = 0.0021$ slug (for two tungsten balls of 0.484 in. diameter; tungsten is chosen for its high density), and $n = 0.65$ sec^{-1} or $c = 0.00193$ lb-sec/ft (corresponding to neon gas, which is chosen for its high viscosity). [Note: For a tuned damper with $1/e$ damping time as given in (38), a gas with low viscosity should preferably be used.]

It is necessary that the theoretical $1/e$ characteristic time τ_p of the untuned concave damper should be compared with experimental results for the following reasons. Formula (33) is obtained from the linearized analysis of the motion of the ball under the assumptions of small amplitude of the motion and an axisymmetric spinning body. In the actual

case, the Telstar satellite is dynamically not axisymmetric. Also, as the tube is limited in length, bottoming will occur when the precession angle is larger than about 3.5°; the motion of the ball will then be disturbed and will not follow (26). An experiment has been devised by G. T. Kossyk which consists of an air-bearing supported flywheel ($I_z = 5.14$, $I_{max} = 4.675$, $I_{min} = 4.404$ slug-ft^2) mounted with two precession dampers as shown in Fig. 5. The flywheel is driven to reach a certain initial speed about a skew axis making a desired angle with the axis of symmetry, which is the principal axis of maximum moment of inertia. As soon as the drive is released, the spinning flywheel performs a preces-

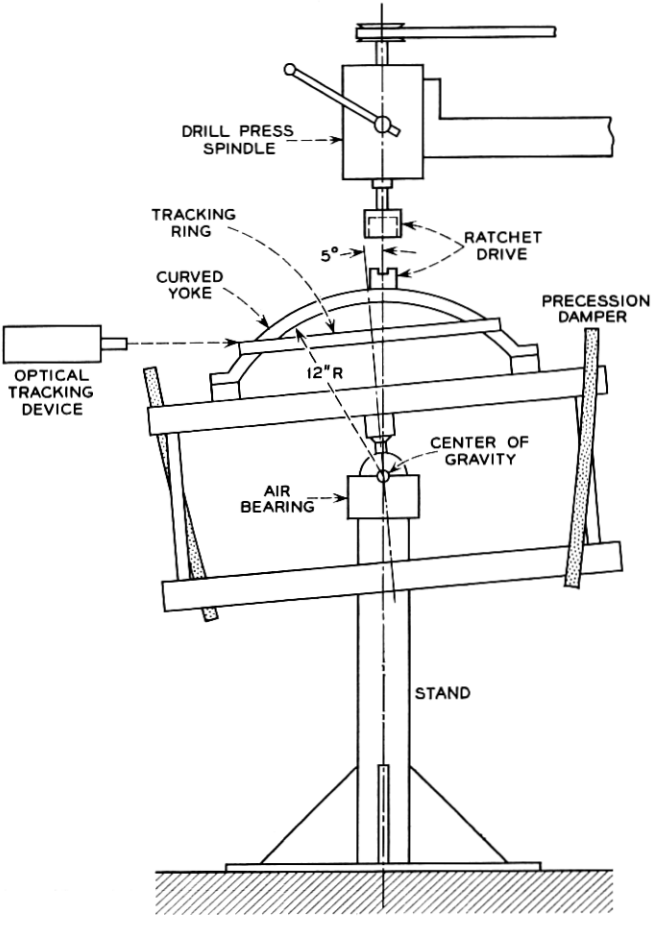

Fig. 5 — Schematic layout of precession damping experiment.

sional motion with known initial angular speed and initial precession angle. The decay of the precession angle is recorded through an optical tracking device for two different cases, with and without the balls in the damper tubes. The difference between these two recordings is the net effect due to the precession damper, excluding all other effects due to air resistance, gravity, etc. The balls were observed to be moving, and bottoming was clearly heard. The experimentally determined τ_p is found to be about four times larger than the theoretical τ_p calculated on the flywheel based on the mean value of the transverse moments of inertia and about nine times larger based on the minimum transverse moment of inertia. Although the Telstar satellite has different moments of inertia from those of the flywheel and a higher $I_{\max}/I_z$ ratio, it is believed that the actual τ_p should not be greater than the theoretical τ_p in (33) by more than one order of magnitude.

For a conservative estimate of the precession damping time of the Telstar satellite, let us multiply (33) by a factor of nine and use the following physical constants: $I_z = 4.1412$, $I_{\max} = 3.8252$ slug-ft^2, $\lambda_{\min} = I_z/I_{\max} = 1.08$, $m = 0.0021$ slug, $n = 0.65$ sec^{-1}, $R = 15$ ft, $b = 1.046$ ft. Equation (33) is then reduced to

$$\tau_p = 19\left(0.76 + \frac{4.35}{\omega_z^2}\right) \text{ minutes}$$

which is relatively independent of the spin rate in the range of interest. At 178.33, 65, and 24 rpm, the maximum $1/e$ characteristic precession damping times are 14.8, 16.2, and 27.6 minutes, respectively.

IV. DRIFT OF SPIN AXIS

We have shown in the Section III that the major transverse torque causing spin precession is contributed by the residual magnetic dipole moment along the spin axis, **M**. (**M** is found to be pointing toward the rocket-mount end of the Telstar satellite.) The torque produced by the residual magnetic dipole moment normal to the spin axis is mostly averaged out because of the spinning motion; other transverse torques, produced by eddy currents and gravity, are all one order of magnitude smaller than that produced by **M**, as shown previously. Therefore, in the qualitative analysis of the spin-axis drift in this section it is sufficient to take only **M** into account.

The initial direction of the Telstar satellite spin axis on the day of launch was 82.3° right ascension and −65.6° declination, as represented by the initial angular momentum, $\mathbf{J}_0$, (see Fig. 1) in the nonrotating coordinate system O-XYZ, where OX points toward the vernal equinox

and OZ is along the earth's spin axis. The geomagnetic field, as shown schematically in Fig. 1, is rotating about OZ at the earth's spin rate. When the satellite is traveling along its orbit, it finds that the geomagnetic induction, **B**, generates a nearly conical surface with respect to $\mathbf{J}_0$ or to O-XYZ, with the axis of the cone pointing in the direction of the orbital angular momentum $\mathbf{J}_{orb}$ (see Fig. 6). Let us pass a plane through O normal to $\mathbf{J}_0$, project the conical surface (or **B**) onto the plane, and construct the time-average resultant of the projection, $\mathbf{B}_\perp$. Then $\mathbf{B}_\perp$ will interact with the magnetic dipole moment **M** (pointing in the negative direction of **J** or ω) to produce a transverse torque, $\mathbf{T}_\perp$, which causes spin precession. Because of the rotation of the geomagnetic field, which has anomalies, and because of the apsidal advance in the orbit, the conical surface generated by **B** has a different area every orbit.

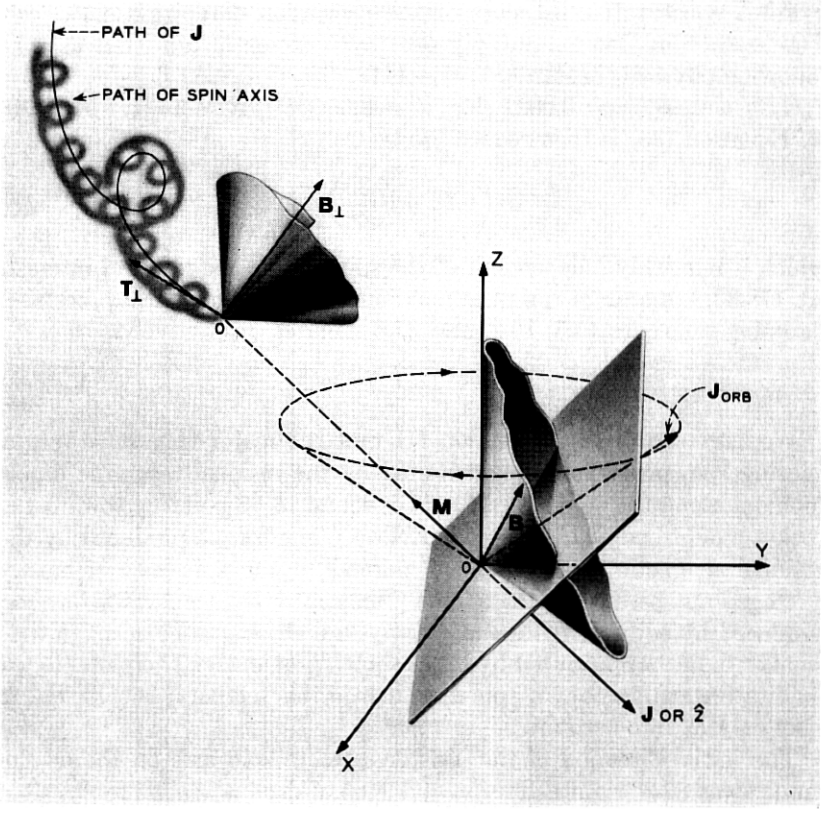

Fig. 6 — Schematic illustration of spin-axis drift.

Furthermore, due to the precession or the nodal regression of the orbital plane, the cone gradually changes its direction in the O-XYZ coordinates, indicated in Fig. 6 as the rotation of $\mathbf{J}_{orb}$ about OZ. As a result, $\mathbf{B}_\perp$ and hence $\mathbf{T}_\perp$ gradually change in both direction and magnitude, while the angular momentum, $\mathbf{J}$, of the satellite follows the pattern of variation of $\mathbf{T}_\perp$, as shown in Fig. 6. Because of spin precession, the spin axis is turning around $\mathbf{J}$, yet does not deviate away from $\mathbf{J}$ as a consequence of precession damping. Therefore, the tip of the spin axis describes a spiral path, shown in an exaggerated way in Fig. 6. Such a phenomenon is termed the drift of the spin axis. The pattern* of the drift is determined by the orbit and by the orientation of $\mathbf{M}$, whereas the rate of drift depends on the orbit and the magnitude of $\mathbf{M}$.

A rough estimate of the rate of drift of the Telstar satellite spin axis can be given. Let us assume that the transverse torque, $\mathbf{T}_\perp$, keeps acting on the satellite perpendicular to the angular momentum, $\mathbf{J}$, despite the fact that $\mathbf{J}$ continuously changes its direction as time goes on. This assumption is justified by the fact that the precession dampers work properly, so that the spin axis is virtually in line with $\mathbf{J}$. Let us disregard the retarding torque at this point. Then, from the principle of angular momentum about the center of mass of the satellite

$$\frac{d\mathbf{J}}{dt} = \mathbf{T}_\perp \tag{39}$$

we find that after a time interval Δt the angular momentum changes to a new position by an angle

$$\Delta\theta = \frac{T_\perp \cdot \Delta t}{J}. \tag{40}$$

In the above we have kept $\mathbf{J} = I_z\omega$, or ω at a constant magnitude, because we have not considered the retarding torque. To evaluate $\Delta\theta$ in a time interval of one week, let us substitute into the above with $\Delta t = 6.048 \times 10^5$ sec, $I_z = 5.61$ kg-m^2, $T_\perp = MH_\perp$, where $M = 0.562 \times 10^{-6}$ weber-meter and $H_\perp = H \cos\gamma$ (H = time-average value of the geomagnetic field on the Telstar satellite orbit and $H_\perp$ is the component of H along the spin axis; γ is the angle between H and the spin axis). Then (40) is reduced numerically to

$$\Delta\theta = 274 \frac{H \cos\gamma}{\omega} \text{ degree}$$

where H is in oersteds and ω in rad/sec. If H is taken to be 0.2 oersted

* For details of the pattern and rate of drift, see Ref. 5.

and γ to be 45°, then at the initial spin rate of 178.33 rpm or $\omega = 18.67$ rad/sec, we find $\Delta\theta = 2.1°$ per week, which is very close to the observed value (approximately 2° per week). This drift rate should increase exponentially with time because of the exponential decay of ω resulting from the action of the retarding torque. It appears from the above estimate that the satellite's residual magnetic dipole moment along the spin axis did not change drastically due to launching.

V. SUMMARY AND CONCLUSIONS

The dynamics problems for the spin-stabilized Telstar satellite, characterized by spin decay, spin-precession damping, and spin-axis drift, have been studied in this paper. In the section on spin decay, the nature of the retarding torque due to eddy-current losses has been analyzed. The observed decay phenomena are largely explained from the computed $\overline{B_\perp^2}$, taking into account the anomalies of the geomagnetic field, the variations of orbital parameters, and the change of the spin-axis direction. The $1/e$ characteristic time of the nearly exponential spin decay is estimated to be about 330 days ±2 per cent by extrapolation from the observed data. This indicates that at the end of two years from the day of launch the Telstar satellite will spin at approximately 20 rpm. It is believed that motion at such a spin rate is still relatively stable with respect to precession.

For the spin precession, it is found that the transverse torque is produced mainly by the residual magnetic dipole moment along the spin axis. The precessional motion of a spinning satellite is illustrated by means of Poinsot's geometrical constructions. A few different types of precession dampers have been considered. Linear analysis of the motion of the ball in the concave type damper has been made, from which explicit expression of the theoretical $1/e$ characteristic precession damping time is obtained. Based on the analysis, it was possible to make a proper design of the damper. An experimental comparison of the theoretical $1/e$ time enables us to estimate the actual $1/e$ time to be about 30 minutes maximum. It is concluded that this damping time is acceptable for the computed magnitude of the transverse torques, and in fact, no precession angle larger than 0.5° has yet been observed on the Telstar satellite.

In discussing the problem of spin-axis drift, only a brief qualitative description is given to illustrate the fundamental mechanism; also, an approximate quantitative analysis is shown for an order-of-magnitude estimate of the drift rate. The observed continuous drift of the spin axis

of the Telstar satellite is evidence of proper functioning of the precession dampers.

The above three problems, which are caused essentially by electromagnetic torques, can be summarized into one of the important dynamics design criteria of a spin-stabilized satellite: i.e., evaluation of the maximum allowable eddy-current losses and residual magnetic dipole moment for specified useful life and orbit of the satellite. Other basic dynamical requirements are worth remarking here. The spin axis should necessarily have a maximum moment of inertia because of provision of precessional energy dissipation and because of elastic energy dissipation, since the satellite is not a perfectly rigid body. This moment of inertia should also be made as large as possible for a given weight and size of the satellite, in order to make the satellite more stable and to increase the lifetime for the same initial spin rate. Furthermore, the ratio of the moment of inertia about the spin axis to those about the transverse axes should be made large enough to yield an adequate precession damping time.

VI. ACKNOWLEDGMENTS

The author wishes to thank J. D. Gabbe for providing various computations of the geomagnetic field, M. S. Glass and D. P. Brady for furnishing data on the measurement of the drag torque and magnetic moment on the Telstar satellites, and G. T. Kossyk for making the precession damping experiments. The author is also indebted to L. Rongved for many useful suggestions in the analysis of precession damping and to J. W. West for various constructive comments and technical advice.

REFERENCES

1. Smythe, W. R., *Static and Dynamic Electricity*, McGraw-Hill, New York, 1950, 616 pages.
2. *Satellite Environment Handbook*, ed. Johnson, F. S., Lockheed Missiles and Space Division, Sunnyvale, California, December 1960, part VIII, Geomagnetism, by Dessler, A. J.
3. Courtney-Pratt, J. S., Hett, J. H., and McLaughlin, J. W., Optical Measurements on the *Telstar* satellite to Determine the Orientation of the Spin Axis and the Spin Rate, Jour. Soc. Motion Picture and Television Engineers, **72**, June, 1963, pp. 462–484.
4. Goldstein, H., *Classical Mechanics*, Addison-Wesley Publishing Co., Cambridge, Mass., 1950, 399 pages.
5. Thomas, L. C., The Long-Term Precession Motion of the *Telstar* Satellite, to be published.